

levels in the melt. The occurrence of well-developed crystals can be explained by the formation of a large number of crystal embryos owing to high ΔT (difference between melt temperature and surface temperature), followed by high crystal growth rate⁵. High crystal growth rate requires high rate of diffusion (mobility) of the atoms/ions/particles in the melt. A high ΔT reduces the viscosity of the melt, thereby hindering growth rate. To counter this, the melt needs to have high volatile content, which will increase the mobility of the components. In the present case, large amounts of CO₂ and SO₂, released during the breakdown of limestone (added as flux during smelting) and sulphide minerals in the ore, may act as volatiles in the melt. The high content of limestone in the ore-feed is indicated by excessively high CaO concentration in the slag (Table 1), while the high FeO concentration suggests the domination of Fe-bearing sulphides, most probably pyrite and chalcopyrite.

Major, minor and trace-element chemistry of slag samples from Bansda and Dhavadiya (Table 1) points to fairly good similarity between slags of the two areas. A definite relationship between the uranium concentrations in the slag vis-à-vis the major element composition could not be established from the data. The most striking feature of the composition is the excessively high content of FeO and CaO in the samples. Although a wide range of possibilities exist to explain the chemical composition of these slags, keeping in mind the local geology dominated by the Archaean basement gneisses and intrusive granites vis-à-vis the probable nature and genesis of the proto-ore, the excess FeO can be interpreted to be originating from Fe-bearing sulphide minerals (pyrite, chalcopyrite, pyrrhotite, etc.), while the excess amount of CaO + MgO can be interpreted to be originating from the limestone added as fluxing material used for smelting the sulphide ore. Keeping in mind the geology and nature of possible host rocks in the vicinity (BGC/metasediments of Bhinder basin/granitic intrusives), the probable host rock seems to be quartz veins in the periphery of a granite intrusive into the TTG gneisses of BGC. This assumption is supported by the occurrence of vein quartz with malachite stains found scattered near the slags.

The high order of radioactivity recorded in the slags of Bansda and Dhavadiya points to the presence of ore-grade uranium concentrations, associated with sulphide mineralization in the vicinity of the basement BGC, intrusive granites and the cover sequence of the Bhinder basin. Though it is not possible to pinpoint the location of mineralization, it is postulated that it is in the immediate neighbourhood of the slag occurrence. Uranium mineralization is closely associated with sulphide minerals, and also with high Cu, Zn and Ni content. The degree as well as extent of radioactivity associated with base metals in the ancient slags of Bansda and Dhavadiya warrant concerted efforts to locate the primary uranium-base metal deposit in the area. This may be achieved by well-

planned geophysical (electrical and/or electromagnetic) surveys in the first phase and drilling in the subsequent phase. Since the probable country rocks are basement gneisses, attempts need to be made to thoroughly investigate the BGC terrain for potential high-grade uranium mineralization.

1. Gupta, P., Ancient orogens of Aravalli region. *Geol. Surv. India. Spec. Publ.*, 2004, **84**, 151–205.
2. Gupta, S. N., Arora, Y. K., Mathur, S. N., Iqbaluddin, Prasad, B., Sahai, T. N. and Sharma, S. B., Geological map of the Precambrian of the Aravalli region. *Geol. Surv. India*, 1995.
3. Bhatt, A. K., Abhinav Kumar and Sundar, G., A note on radioactive and other sulphide slag occurrences and ancient mine workings in Salambar–Banswara area, Rajasthan, India. *J. At. Miner. Sci.*, 1998, **6**, 83–89.
4. Kerr, P. F., *Optical Mineralogy*, McGraw-Hill, New York, 1977, pp. 382–383.
5. Best, M. G., *Igneous and Metamorphic Petrology*, CBS Publishers & Distributors, Delhi, 1986, pp. 237–246.

ACKNOWLEDGEMENTS. We thank the Director, AMD for permission to publish this paper. Thanks are also due to the anonymous referee for his comments.

Received 26 October 2007; revised accepted 13 March 2008

ULF emissions associated with seismic activity recorded at Kolhapur Station

A. K. Sharma*, A. V. Patil, R. N. Haridas and R. V. Bhonsle

Space Science Laboratory, Department of Physics, Shivaji University, Kolhapur 416 004, India

In this communication, we present some observations and preliminary results associated with seismogenic ultra low frequency (ULF) emissions. We have analysed ULF data for two moderate earthquakes that occurred on 17 April and 21 May 2006, with magnitudes greater than 4. For recording ULF data using ground-based method, three induction-coil magnetometers have been installed at Shivaji University, Kolhapur, India (16.40°N, 74.15°E). Data have shown maximum enhancement in intensities of magnetic field for 0.1 Hz, 3–5 days before the earthquakes. Polarization parameter and geomagnetic pulsation in terms of K_p index have been used to conclude that the observed enhancement in magnetic field (before the earthquake) is seismogenic.

Keywords: Earthquakes, electromagnetic emissions, polarization ratio, power spectrum analysis.

EARTHQUAKE prediction is one of the most challenging problems in earth sciences. Association between possible

*For correspondence. (e-mail: sharma_ashokkumar@yahoo.com)

electromagnetic precursors and earthquakes has been recently reported^{1,2}. Earthquakes produce reliable precursors in the ultra low frequency (ULF) band (0.01–30 Hz)^{1,2}. Study of magnetic field anomaly in the ULF range provides significant information regarding the prediction of earthquakes^{3–5}. Possible mechanism of generation of electromagnetic waves in the lithosphere is identified with the microfracturing effect⁶ and electrokinetic effect⁷. Such emissions associated with the rock process are observed in the ULF and high frequency (HF) ranges. ULF signals have precursory time from a few days to several weeks⁸. Studies have reported ground-based observations of ULF/VLF waves associated with seismic activities⁹, and we also report here the same using our system. The data processing was done using MATLAB software for power spectrum analysis. The main aim of our study was to find possible correlation between observed ULF emissions prior to and due to earthquakes.

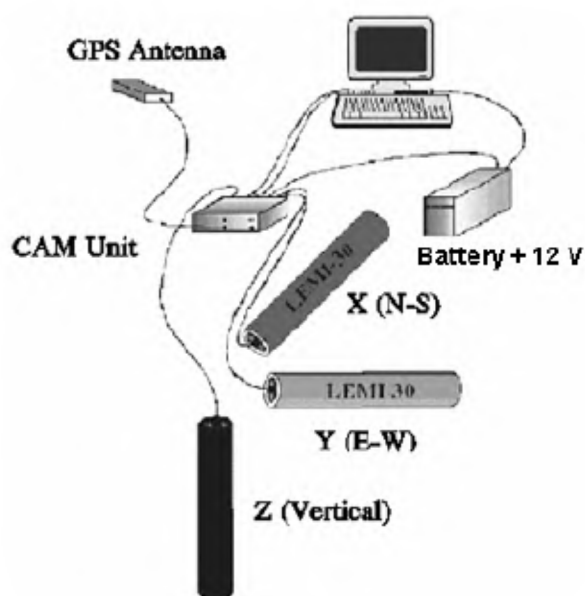


Figure 1. Schematic of experimental set-up of induction-coil magnetometers at Shivaji University, Kolhapur.

Table 1. Technical parameters of the induction coil magnetometer

Frequency band of measured signals	0.01–30 Hz
Transformation factor from	
0.01–1 Hz	$20 \times f \text{ mV/nT}$
1–30 Hz	20 mV/nT
Auxiliary output gain	20 dB
Maximum output signal	$\pm 5 \text{ V}$
Magnetic noise level at	
0.01 Hz	$\leq 20 \text{ pT} \times \text{Hz}^{-1/2}$
0.1 Hz	$\leq 2 \text{ pT} \times \text{Hz}^{-1/2}$
1 Hz	$\leq 0.2 \text{ pT} \times \text{Hz}^{-1/2}$
10–30 Hz	$\leq 0.04 \text{ pT} \times \text{Hz}^{-1/2}$
Temperature range of operation	$-10/50^\circ\text{C}$
Dimensions	$900 \times \phi 100 \text{ mm}$
Weight	6.5 kg

Towards the end of 2005, a magnetic field measurement system was installed in the Shivaji University, Kolhapur (16.40°N, 74.15°E) near Koyna, an earthquake-prone region in western Maharashtra, India. Figure 1 shows the schematic set-up of an induction coil magnetometer. It consists of three induction-coil magnetometers (LEMI-30i) in orthogonal directions (east-west, north-south and vertical) having length 1 m each. It is used to measure the variation in magnetic field in the range 0.01–30 Hz. These magnetometers measure magnetic field components namely B_x , B_y and B_z . GPS antenna provides information about latitude, longitude, altitude of the site and universal time. LEMI 30i Logger is used for recording data from induction-coil magnetometers, acquired by the CAM unit, and to handle the commands to the CAM unit through its graphical-user interface. The data from each magnetometer are digitized at the sampling rate of 64 Hz and recorded hourly on a hard disc. Such an ULF system has already been discussed in detail earlier¹⁰. Technical parameters of the induction coil magnetometer are given in Table 1.

In the present study, earthquake information retrieved (from USGS website) for the two moderate earthquakes has been used. ULF data of magnetometers was obtained for 0.1 Hz for the two earthquakes, about 15 days before and a few days after the mainshock for 10 h during night (14:00–23:00 UT) to avoid man-made noise and geomagnetic pulsation, etc. In 2006, our system observed two moderate earthquake events. The first occurred on 17 April 2006 (epicentre at Satara, 17.2°N, 74.0°E) at 16:40 UT (magnitude (M_b) and depth were 4.4 and 10 km respectively); the second one occurred on 21 May 2006 (epicentre at Ratnagiri, 16.8°N; 73.7°E) at 20:28 UT (magnitude (M_b) and depth were 4.2 and 34 km respectively). Power-spectrum analysis of the data was done using MATLAB software. This analysis gives temporal variation in intensity of the magnetic field at 0.1 Hz. The polarization ratio analysis was performed to discriminate geomagnetic pulsation from ULF noise due to the earthquake. Contribution of solar particle radiation was examined using K_p index data obtained from World Data Center, Kyoto, Japan available on the internet (<http://swdcwww.kugi.kyoto-u.ac.jp/kp/index.html>). In both the cases, we observed the electromagnetic emissions associated with seismic activity.

Figures 2–5 show the temporal variations in intensities of magnetic field from 14:00 to 23:00 UT at 0.1 Hz for April and May 2006 respectively. The ordinates show emission intensities of magnetic field and abscissa show dates. The value of maximum magnetic field intensity observed on 11/12 April was $0.004594 \text{ nT}^2/\text{Hz}$ (five days before the mainshock), whereas the normal magnetic field intensity for other days of this month was about $0.00002397 \text{ nT}^2/\text{Hz}$. This is about 115 times larger than the normal intensity of the magnetic field (Figure 2). Figures 3 and 6 show polarization ratios for April and May 2006 respectively. Polarization parameter helps to distinguish between geomagnetic pulsation and seismogenic

emissions. Generally, polarization ratio is around 1 for intense seismo-magnetic emission, whereas it might decrease during magnetic storm time. Figures 3 and 6 show polarization ratios¹¹ around 1, implying that the observed enhancement in magnetic field is due to the ULF emission during (and even before) the seismic activity. Figures 4 and 7 show geomagnetic pulsation in terms of Kp index for April and May 2006 respectively. Kp is a planetary geomagnetic activity¹¹, and its value lies in the range 0–9. ΣKp is the sum of three hourly values of Kp . $\Sigma Kp < 30$ indicates quiet magnetic activity (and $\Sigma Kp > 40$ indicates strong disturbance in the magnetic activity)¹². For 9 and

and 14 April, ΣKp values were 38 and 43 respectively. But there was negative correlation between seismogenic emissions and geomagnetic pulsation. Therefore polarization ratios, ΣKp values and negative correlation between geomagnetic pulsation and seismogenic emission indicate that the enhancement observed in magnetic field intensity on 11/12 April was seismogenic.

Similarly, the value of maximum magnetic field intensity observed on 17/18 May was $0.002513 \text{ nT}^2/\text{Hz}$ (three days before the mainshock), whereas the normal magnetic field intensity for the month was about $0.00005740 \text{ nT}^2/\text{Hz}$. This is about 48 times larger than the normal intensity of magnetic field (Figure 5). (However on 23 May also some enhancement had been observed.) Geomagnetic activity was quiet, as during May 2006, ΣKp values were below 30.

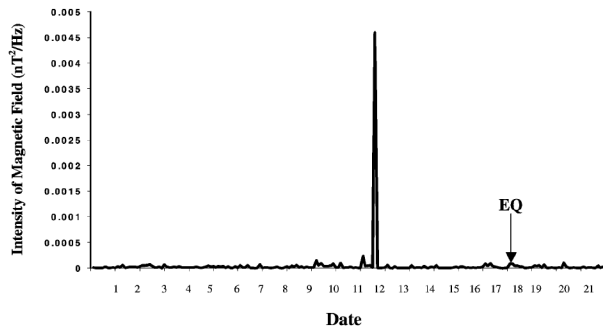


Figure 2. Temporal variation in magnetic field at 0.1 Hz from 1 to 21 April 2006.

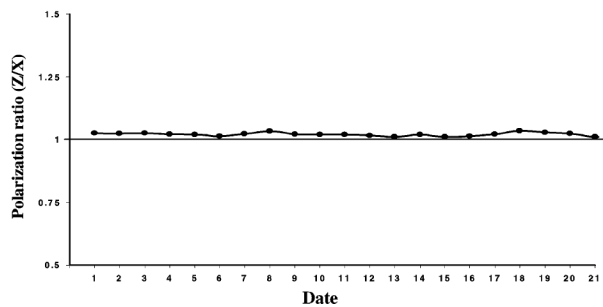


Figure 3. Variation in polarization ratio from 1 to 21 April 2006.

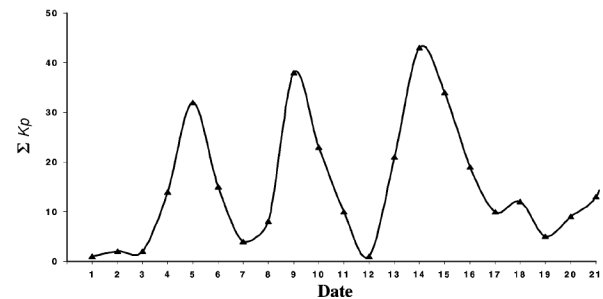


Figure 4. Geomagnetic pulsations in terms of Kp index from 1 to 21 April 2006.

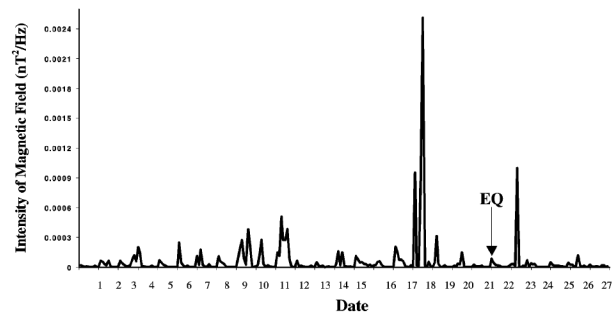


Figure 5. Temporal variation in magnetic field at 0.1 Hz from 1 to 27 May 2006.

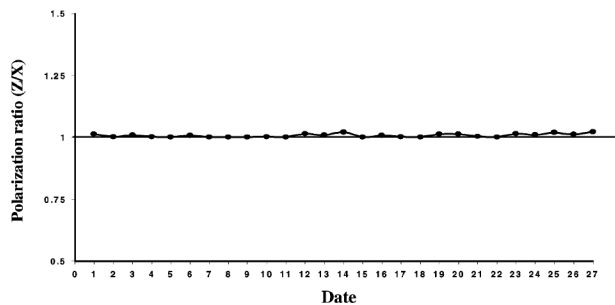


Figure 6. Variation in polarization parameter from 1 to 27 May 2006.

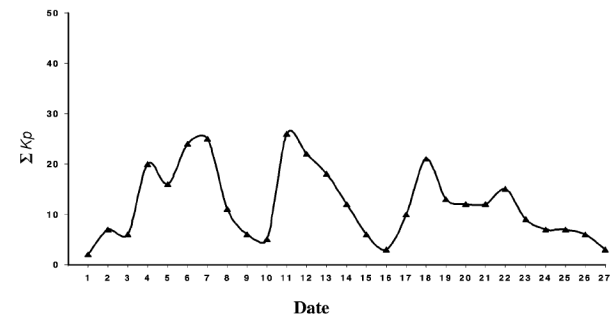


Figure 7. Geomagnetic pulsation in terms of Kp index from 1 to 27 May 2006.

As has been discussed above, large enhancements were observed on 11/12 April and 17/18 May 2006 for the moderate earthquakes that occurred on 17 April and 21 May 2006. These enhancements were many times larger (about 115 and 48 times respectively) than the background for the respective months. On the basis of polarization ratios and also due to the use of night-time data, we conclude that these observed enhancements are, perhaps, seismogenic. Moreover, during these periods the geomagnetic activity was also low.

In the present case, we could observe large and convincing enhancements in magnetic-field intensities, 3–5 days before the occurrence of moderate, and nearby, earthquakes. This suggests that these enhancements can be treated as precursory signatures of the impending earthquakes. This may lead to short-term prediction of earthquakes.

However, we suggest that before establishing this technique beyond doubt, similar exercise may be undertaken on the basis of large database of moderate and strong earthquakes that might have occurred with nearby and distant epicentres.

Japan, possibly associated with the Chi-chi earthquake in Taiwan. *Ann. Geophys.*, 2005, **23**, 1335–1346.

12. Hattori, K., Akinaga, Y., Hayakawa, M., Yumoto, K., Nagao, T. and Uyeda, S., ULF magnetic anomaly preceding the 1997 Kago-shima earthquakes. In *Seismo Electromagnetics: Lithosphere–Atmosphere–Ionosphere Coupling* (eds Hayakawa, M. and Molchanov, O. A.), Terr. Sc. Publ., Tokyo, 2002, pp. 19–28.

ACKNOWLEDGEMENTS. We thank the Department of Science and Technology, New Delhi for providing financial support through a project. Thanks are due to Dr R. S. Vhatkar and P. T. Patil for help during installation of the system. We also thank the referees for useful comments to revise the manuscript.

Received 19 February 2007; revised accepted 26 February 2008

Extreme rainfall events: Vulnerability analysis for disaster management and observation system design

P. Goswami* and K. V. Ramesh

CSIR Centre for Mathematical Modelling and Computer Simulation, Wind Tunnel Road, Bangalore 560 037, India

Extreme rainfall events today pose a serious threat to many populated and urbanized areas worldwide. An accurate estimate of frequency and distribution of these events can significantly aid in policy planning and observation system design. We report here a high-resolution (10 km) analysis of heavy rainfall episodes (defined as 24-h rainfall exceeding 250 mm) over the Indian region. The dataset, recently developed by NOAA, USA, provides daily composite rainfalls for the period 2001–06 at locations approximately 10 km apart. We first assess the reliability of the dataset by comparing it with daily gridded ($1^\circ \times 1^\circ$) rainfall data from IMD and three-hourly gridded ($0.25^\circ \times 0.25^\circ$) data from TRMM for the overlap years (2001–04). A category-wise analysis of the high-resolution data reveals a number of hotspots of vulnerability; in particular, the semiarid region in northwest India emerges as a high-vulnerability area in terms of extreme rainfall events. The high-resolution analysis also clearly reveals the corridor of the monsoon trough, lined by a flower-pot distribution of extreme rainfall events along the flanks. This can be a valuable input for precision design of field experiments on the continental trough or on localized extreme events like thunderstorms. Other important implications for areas like vulnerability assessment, planning and mesoscale forecasting are discussed.

Keywords: Disaster management, extreme rainfall events, forecasting, vulnerability analysis.

*For correspondence. (e-mail: goswami@cmmacs.ernet.in)

1. Hayakawa, M., Hattori, K. and Ohta, K., Monitoring of ULF geomagnetic variations associated with earthquakes. *Sensors*, 2007, **7**, 1108–1122.
2. Koptenko, Y., Ismagilov, V., Hayakawa, M., Smirnova, N., Troyan, V. and Peterson, T., Investigation of the ULF electromagnetic phenomena related to earthquakes: Contemporary achievement and the perspective. *Ann. Geofis.*, 2001, **44**, 325–334.
3. Hayakawa, M., Kawate, R., Molchanov, O. A. and Kiyohumi, Y., Results of ultra-low-frequency magnetic field measurements during the Guam earthquake of 8 August 1993. *Geophys. Res. Lett.*, 1996, **23**, 241–244.
4. Faser-Smith, A. C., McGill, P. R., Helliwell, R. A. and Villard Jr O. G., Ultralow-frequency magnetic field measurements in southern California during the Northridge earthquake of January. *Geophys. Res. Lett.*, 1994, **21**, 2195–2198.
5. Hayakawa, M., Ito, T., Hattori, K. and Yumoto, K., ULF electromagnetic precursors for an earthquake at Biak, Indonesia on 17 February 1996. *Geophys. Res. Lett.*, 1996, **27**, 1531–1534.
6. Molchanov, O. A. and Hayakawa, M., Generation of ULF electromagnetic emission by microfacturing. *Geophys. Res. Lett.*, 1995, **22**, 3091–3094.
7. Bhattacharya, S., Shrivastava, A. and Gwal, A. K., Ground-based methodology for determining ultra low frequency (ULF) electromagnetic emissions associated with seismic activity. In IAGA WG1.2 on Electromagnetic Induction in the Earth Proceedings of the 17th Workshop, Hyderabad, India, 2004.
8. Eftaxias, K., Kaporis, P., Olygiannakis, J., Peratzakis, A., Kopanas, J., Antonopoulos, G. and Rigas, D., Experience of short term earthquake precursors with VLF–VHF electromagnetic emissions. *Nat. Hazards Earth Syst. Sci.*, 2003, **3**, 201–228.
9. Parrot, M., The micro-satellite DEMETER. *J. Geodyn.*, 2002, **33**, 535–541.
10. Kushwah, V., Vikram Singh, Birbal Singh and Hayakawa, M., Ultralow frequency (ULF) magnetic field anomalies observed at Agra and their relation to moderate seismic activities in Indian region. *J. Atmos. Sol.-Terr. Phys.*, 2005, **67**, 992–1001.
11. Hayakawa, M., Ohta, K., Nickolaenko, A. P. and Ando, Y., Anomalous effect in Schumann resonance phenomena observed in